Available online at www.sciencedirect.com
SCIENCE DIRECT®
Cement and Concrete Research 35 (2005) 2143 – 2157
Cement and Concrete Research

Comparison of solidification/stabilization effects of calcite between Australian and South Korean cements

Dongjin Lee [a], T. David Waite [a,*], Gareth Swarbrick [a], Sookoo Lee [b]

[a] School of Civil and Environmental Engineering, The University of New South Wales, Sydney, NSW 2052, Australia
[b] School of Environmental Engineering, The Seoul National University of Technology, Nowon-Gu, Seoul, 139-743, Korea

Received 21 August 2002; accepted 10 November 2003

Abstract

The differences in the effect of calcite on the strength and stability of Pb-rich wastes solidified and stabilized using Australian and South Korean ordinary Portland cements are examined in this study. Pb-rich waste stabilized using Australian OPC has been shown to possess both substantially higher unconfined compressive strength and lead immobilization ability than South Korean OPC as a result of its higher C_3S content and the associated enhanced degree of precipitation of lead on the surfaces of silicate phases present. Calcite addition is observed to have an accelerating effect on the OPC-induced solidification/stabilization of Pb-rich wastes as gauged by the unconfined compressive strength and leachability of the solids formed. This effect is observed to be far more dramatic for South Korean OPC than for Australian OPC. Using scanning electron microscopy, waste stabilized with cement and calcite was observed to develop significantly greater proportions of hydrated crystals than wastes stabilized with cement alone. The results of X-ray diffraction studies have shown that the presence of calcite in South Korean OPC results in greater acceleration in the formation of portlandite than is the case for Australian OPC.

Keywords: Portland cement; $CaCO_3$; Lead; Compressive strength; X-ray diffraction

1. Introduction

The quantity of hazardous waste, radioactive waste and contaminated land has increased with the development of industrial activities in many parts of the world. Solidification is a recognized technique for stabilization of these wastes prior to disposal with common methods including cement and lime based techniques, glassification, thermoplastic techniques, and encapsulation [1]. The use of Portland cement for solidification/stabilization (S/S) processes has been considered particularly suitable for the treatment of hazardous wastes due to its relatively low cost and demonstrated effectiveness over many years [1,2]. Because cement can convert mobile dust, liquids, and sludges to a monolithic solid form, its use potentially prevents pollutants from migrating into the environment by rendering the toxic contaminants physically immobile and chemically bonded to the encapsulating solid.

The S/S of hazardous wastes has been studied with particular interest exhibited in methods of improving the stability of solidified forms, particularly in view of possibilities of reuse of these waste materials [3]. A variety of agents have been found to substantially improve the characteristics of the solid waste forms (SWFs) generated from cement-based S/S. For example, calcite has been found to potentially induce an increase in strength of the SWF and to decrease the leachability of heavy metals. The present work constitutes part of a collaborative investigation, undertaken in Australia and Korea, into the effect of calcite on S/S processes. It was found in preliminary studies using Korean ordinary Portland cement (OPC), that strength was markedly improved by the addition of calcite but subsequent studies using Australian OPC showed much less dramatic improvement. It is hypothesised that the observed differences are due to the different composition of the two cements.

The effects of different cement types on S/S of heavy metals have been extensively examined in recent years. The typical

* Corresponding author. Tel.: +61 2 9385 5793; fax: +61 2 9385 6139.
E-mail address: d.waite@unsw.edu.au (T.D. Waite).

0008-8846/$ - see front matter © 2005 Elsevier Ltd. All rights reserved.
doi:10.1016/j.cemconres.2005.08.008

Table 1
Typical mineralogical composition of Portland cements [2]

Cement type		C_3S	C_2S	C_3A	C_4AF	$CaSO_4$	MgO
I	Ordinary Portland	45	27	11	8	3.1	1.4
II	Moderate heat evolution	44	31	5	13	3.8	2.5
III	High early strength	53	19	11	9	4.0	2.0
IV	Low heat evolution	28	49	4	12	3.2	1.8
V_a	Sulfate resistant	38	43	4	9	2.7	1.9
V_b	Rapid hardening	66	11	8	9	4.2	1.1
V_c	Super rapid hardening	68	5	9	8	5.1	2.0

Table 3
The chemical and mineralogical composition of Australian and Korean cements used in this study

Australian cement				Korean cement			
Compound	%	Mineral	%	Compound	%	Mineral	%
CaO	64.5	C_3S	66.4	CaO	62.4	C_3S	41.7
SiO_2	20.2	C_2S	8.1	SiO_2	20.7	C_2S	27.9
Al_2O_3	4.4	C_3A	4.4	Al_2O3	6.8	C_3A	12.7
Fe_2O_3	3.6	C_4AF	11.0	Fe_2O_3	3.1	C_4AF	9.4
SO_3	3.0	$CaSO_4$	5.1	SO_3	1.7	$CaSO_4$	2.9
MgO	1.5			MgO	3.3		

mineral composition of Portland cement types is given in Table 1, and the physical properties of different cements [4] are shown in Table 2. Conner [2] investigated the leachability of a number of solidified waste samples by cement types I and II. Most heavy metals were fixed relatively well in Type I but immobilization of Zn was slightly better in Type II than in Type I. The effect of differences in composition between Type I cement and Calcium Aluminate Cement (CAC) on the S/S of hazardous wastes has been examined by Murat and Sorrentino [5]. They have argued that Type I can absorb a large amount of Cd and Zn while CAC easily traps Cd and Cr. It was indicated that differences of composition between Type I cement containing silicate-rich minerals and CAC containing aluminate-rich minerals resulted in different mineralogical composition of the SWF with each of the heavy metals and, as a result, different leachabilities.

Five types of cement, Type I, White Ordinary Portland Cement (WOPC), Type V_a, Type V_b, and CAC, were used to investigate the influence of carbonation on the S/S of hazardous wastes [6]. SWF with these five cements showed an increase in strength when cured in an environment of carbon dioxide compared to those under normal atmospheric conditions. In particular, Type V_b achieved the highest strength cement in the absence and presence of waste addition with curing in nitrogen and in ambient as well as in carbon dioxide environments. It was found that WOPC and Type I have the lowest leachability for the treatment of chromium, Type V_a for arsenic and Type I for copper.

The purpose of this study is to examine the difference in the S/S response of two cements, cement-A (Australian) and cement-K (Korean), and to assess the hypothesis that differences in behaviour can be attributed to the difference in composition of these cements. Of particular interest is the effect of calcite in enhancing the S/S of Pb-doped wastes. Compressive strength and leaching tests were the primary tools used to compare the effectiveness of SWF produced, and electron microscopic image analysis and X-ray diffraction were used to identify the solidified products.

2. Materials and methods

2.1. Materials

In this study, Australian general purpose Portland cement (AS3972-1997) (denoted cement-A) and Sangyong normal Portland cement (denoted cement-K) were used. Chemical and mineral compositions of cement-A and cement-K are indicated in Table 3. High grade crystalline calcite ($\geq$95.0% $CaCO_3$, $\leq$4.0% $MgCO_3$ and $\leq$1.5% acid insolubles) was used as the cement additive while "synthetic" Pb-rich waste was prepared from a lead nitrate hydroxide paste. The lead nitrate hydroxide paste was prepared from lead nitrate that was precipitated to form hydroxide sludge by adjusting the pH to 8.5 with 6.0 N sodium hydroxide. The paste was dried at 104 °C prior to use.

Various ratios of dry Pb waste, calcite and cement were mixed with water at a water/cement ratio of 0.3. After thorough mixing the samples were introduced into polyethylene cylindrical moulds measuring 20 mm diameter internally and 40 mm in height. After 24 h the samples were removed from the mould and curing was carried out in humid air at 20 °C for 7, 14, 28 and 60 days. Samples were prepared in triplicate and are denoted Cal*i*,Pb*j*-K and Cal*i*,Pb*j*-A where *i* is the calcite content, *j* is the Pb-doped waste content, -K refers to Korean cement and -A to Australian cement. A summary of mixtures used and their associated notation is given in Table 4.

2.2. Methods

2.2.1. Unconfined compressive strength (UCS)

UCS testing was undertaken on the samples using an Instron testing machine. The top and bottom of the samples was capped with Masonite® to limit the effect of cracking. Loading was

Table 2
Typical setting times and compressive strengths for Portland cement types [4]

Cement type	Setting time (min)		Compressive strength (kgf/cm^2)			
	First	Last	1 day	3 days	7 days	28 days
Type I: Ordinary Portland	147	209	–	143	239	409
Type II: Moderate heat evolution	198	277	–	96	153	330
Type V_a: sulfate resistant	170	237	–	129	190	336
Type V_b: rapid hardening	121	195	125	245	340	460

Table 4
Summary of mixture nomenclature used in this study

	Calcite 0%	Calcite 5%	Calcite 10%
Pb waste 0%	Cement cement-A/K	Cal5-A/K	Cal10-A/K
Pb waste 5%	Pb5-A/K	Cal5,Pb5-A/K	Cal10,Pb5-A/K
Pb waste 10%	Pb10-A/K	Cal5,Pb10-A/K	Cal10,Pb10-A/K
Pb waste 20%	Pb20-A/K	Cal5,Pb2,cement-A/K	Cal10,Pb20

increased until maximum load was achieved and visible cracks appeared. The compressive strength was calculated as the maximum applied load divided by the cross-sectional area [7].

2.2.2. Leaching procedure

Leaching tests were carried out on samples that had been cured for 30 days using the US EPA Toxicity Characteristic Leaching Procedure (TCLP) [8]. Samples were ground to particles of a size able to pass through a 9.5 mm standard sieve (i.e. of size less than approximately 1 mm) and leached with acetic acid at pH 4.93±0.05. The solid phase was extracted with an amount of extraction fluid equal to 20 times the weight of the solid phase. The samples were agitated in a rotary tumbler at 30 rpm for 18 h. The extract was separated from the solid phase by 0.6–0.8 ìm pore size glass fibre filtration. A Perkin-Elmer 4000 Inductively Coupled Plasma (ICP) was used to determine metal concentrations in the leachate.

2.2.3. Scanning electron microscopy (SEM)

Scanning electron microscope images were obtained using a Hitachi 4500 SEM fitted with electron dispersive spectroscopy (EDS). Samples for SEM analysis were cured for 28 days and then dried at 104 °C for 24 h. The dried solid samples were carefully ground then coated with carbon to prevent electronic charging effects during the SEM analysis.

2.2.4. X-ray diffraction (XRD)

The mineralogical composition of the samples was analysed using Cu K_α radiation at 35V and 25 mA on a Philips 1830 XRD diffractometer. XRD scans were obtained using 0.04° steps with 2 s counting time.

2.2.5. Solution analysis of cement slurries

Cement slurries with a water/cement ratio of 2 were prepared and the concentrations of ions in aqueous solutions of these cement slurries were measured as a function of time up to 30 min after slurry preparation. The slurry solutions were filtered with fine grade Whatman No. 50 filter papers prior to analysis of the filtrate by a variety of methods. All experiments were carried out at an ambient temperature of 22±2 °C. The analytical methods used are as follows:

(i) Ca, Al, Fe, Pb, K, Mg and Si were determined by Inductively Coupled Plasma Atomic Emission Spectroscopy (ICP-AES). All samples were acidified using nitric acid and diluted for the analyses according to the detection limits suggested in APHA/AWWA Standard Methods (1995) [9]. Silicon was separately analysed because silica readily precipitates in acidic solutions.
(ii) SO_4^{2-} was determined using a standard turbidimetric method [9] in which barium chloride ($BaCl_2$) was added to induce barium sulfate precipitation. Any suspended matter present was removed by filtration prior to turbidimetric analysis to improve the accuracy of the test.
(iii) CO_3^{2-} content was determined by measuring the phenolphthalein alkalinity (P) and total alkalinity (T) in the range of $P>1/2T$ (pH above 12.5) ($[CO_3^{2-}]=2(T-P)$).

3. Results

3.1. Effect of calcite on the UCS of cement-A and cement-K

The results of UCS measurements on cement-A and cement-K in the absence and presence of calcite over 2 months of curing time are shown in Fig. 1. Cement-A attains a compressive strength of over 9000 N/cm^2 within 14 days of

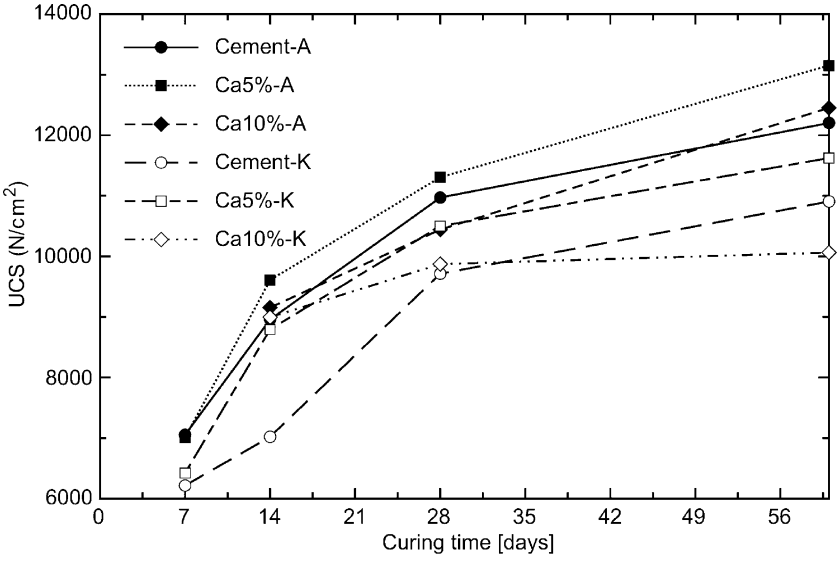

Fig. 1. Compressive strength in the absence and presence of calcite between cement-A/cement-K.

curing and approximately 11,000 N/cm^2 after 28 days of curing. Cement-K develops a strength of around 7000 N/cm^2 at 14 days and only 9500 N/cm^2 after 28 days. In cement-A, strength development with 5% calcite (Cal5-A) is observed to be slightly superior to that without calcite. Cement-A with 10% calcite (Cal10-A) provides the same strength as regular cement-A after curing for 60 days. For cement-K, 5% calcite addition (Cal5-K) is observed to yield similar strength to cement-K at 7 days, exhibits a markedly higher strength at 14 days, and then attains a slightly higher strength at 60 days. Early strength development in cement-K containing 10% calcite is observed to be almost the same as that with 5% calcite with little increase over the following 2 months.

3.2. UCS development in cement-A and cement-K containing Pb

The results of UCS measurements on cement-A in the absence and presence of Pb over 60 days of curing time are shown in Fig. 2a. Regular cement-A alone attains a compressive strength of over 6000 N/cm^2 within 7 days of curing while cement-A with 10% lead addition (Pb10-A) has almost no compressive strength at 7 days. The strength of 10% Pb-doped cement-A attains up to 70% of that of regular cement (cement-A) at 14 days, and approximately 80% at 60 days. Strength development in 5% Pb-doped cement-A is observed to be slightly lower than that of regular cement-A over 2 months. The hydration of cement-A with 20% Pb is significantly retarded after 14 days of curing, and then markedly increases up to almost the same strength as that of 10% Pb-doped cement-A at 60 days. The results also indicate that there is still some ongoing strength development at 60 days.

Fig. 2b shows the effect of Pb in inducing poor strength development in cement-K with the retardation effect obviously substantially stronger than observed for cement-A. The strengths in all cement-K samples containing Pb are essentially zero up to 14 days, but increase to 20% (40% in Pb5-K) of that for pure cement-K at 28 days. Pb10-K and Pb20-K achieve a

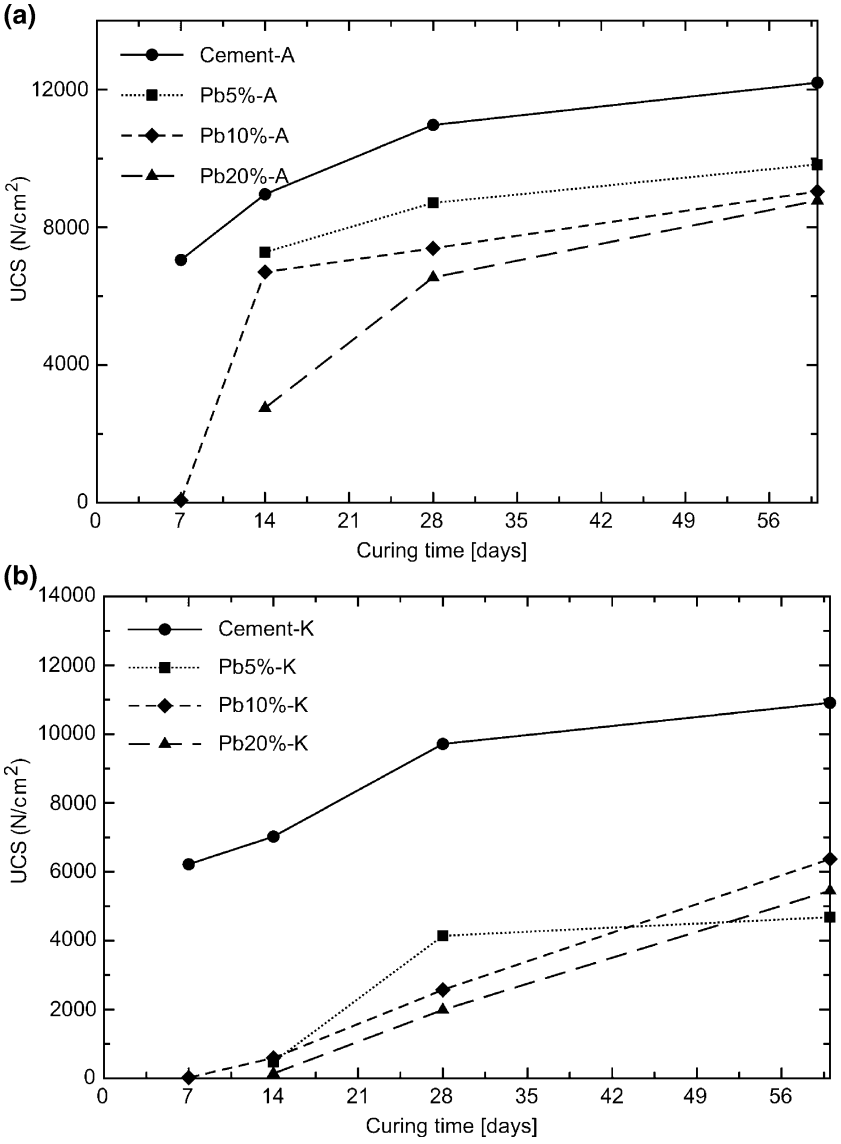

Fig. 2. Compressive strength in the absence and presence of lead wastes. (a) Australian cement: (b) Korean cement.

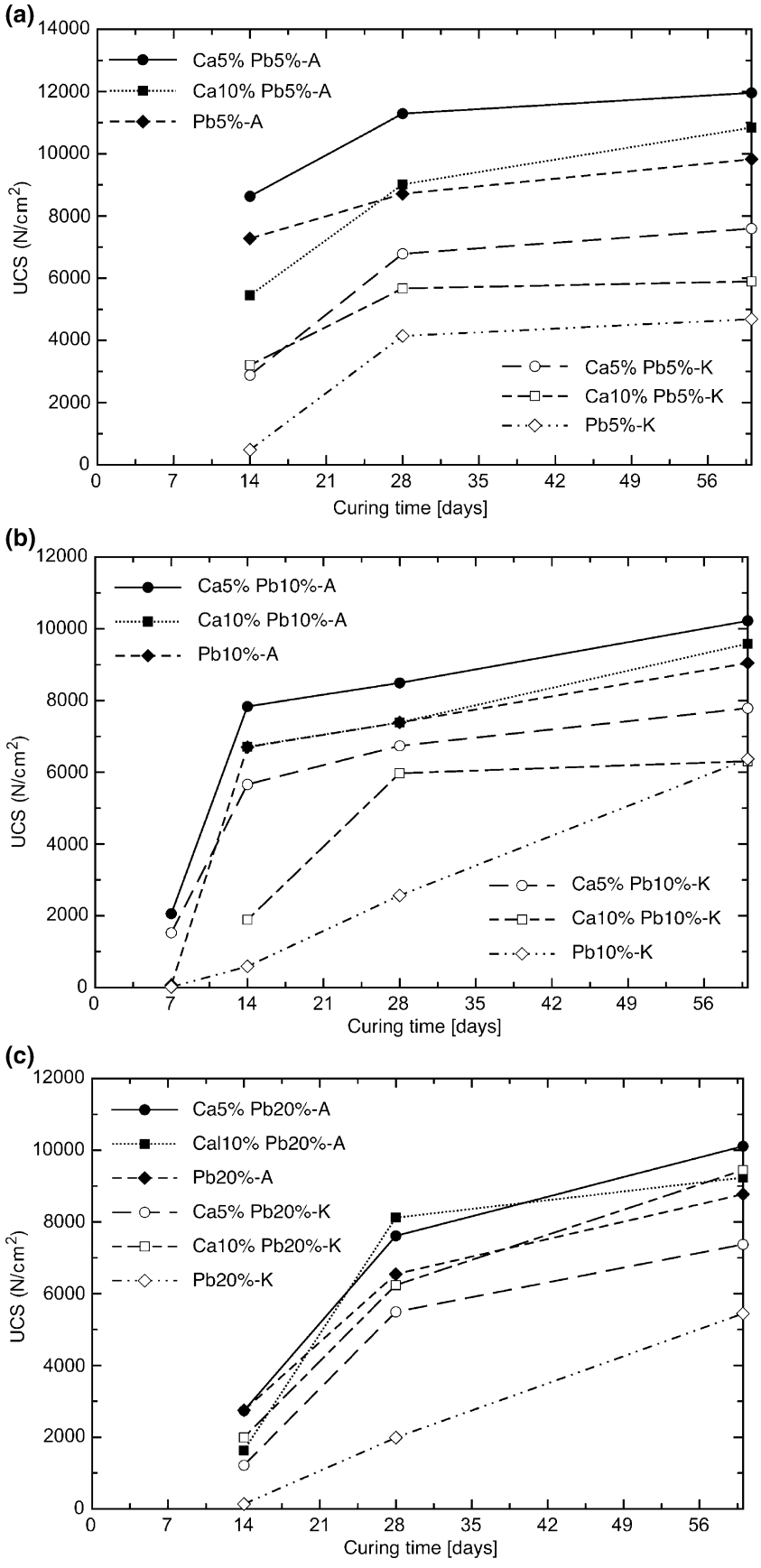

Fig. 3. Comparison of calcite effect between cement-A/cement-K. (a) on 5% lead addition: (b) on 10% lead addition: (c) on 20% lead addition.

UCS of 40% of regular OPC after 60 days and appear to continue to gain some strength thereafter.

3.3. UCS of Pb-doped SWFs in the presence of calcite

The UCS of Pb-doped SWF generated using cement-A and cement-K in the presence of calcite is shown in Fig. 3. For cement-K, all Pb doped samples in the absence of calcite have almost no compressive strength in the first 14 days of curing and can, in general, only withstand on the order of 2000 N/cm^2 at 28 days. Additions of calcite, however, are observed to partially rectify this poor strength development with a UCS of approximately 3000 N/cm^2 at 14 days and about 6000 N/cm^2 at 28 days. Strength developments in 5%~10% Pb-doped SWF to which 5% calcite has been added are always observed to be slightly superior to those of 10% calcite addition. The addition of 10% calcite in 20% lead-doped samples yields a slightly stronger UCS than with only 5% calcite. In particular, strength development of Cal10,P20-K is observed to be more than twice that of P20-K at 60 days.

In all cases use of cement-A results in superior strength development for all combinations of lead and calcite addition. In SWFs with 5% and 10% lead, 10% calcite addition is found to attain almost the same or slightly higher strength compared to those in the absence of calcite, and, in SWFs with 20% lead, the presence of 10% calcite also yields SWFs of similar strength at 14 days to SWFs without calcite. In all lead-doped materials, additions of 5% calcite are observed to yield strengths that are 10%~20% above those observed in the absence of calcite.

Fig. 4 shows the relative performance of solidified Pb-doped wastes containing calcite compared to that of pure cement at 28 days. It is clear that 5% calcite addition provides the best strength recovery and, in the case of Cal5,Pb5-A, supersedes that for cement alone (cement-A). It is also evident that cement-K is much more susceptible to strength reduction due to the presence of lead than cement-A.

3.4. Leachability of Pb-doped SWFs generated using cement-A and cement-K

TCLP extraction tests were used to quantify the leachability of lead and other analytes from the SWFs. The results for lead for all samples are plotted in Fig. 5. The total concentrations of lead present in the leach mixtures for (non-solidified) 5%, 10% and 20% Pb-doped wastes are 1925, 3930, and 7860 mg/l, respectively. Lead concentrations in the extraction fluid for 5%, 10% and 20% lead-doped materials solidified by cement-K alone (i.e. no calcite addition) are 79.2, 388.0, and 1,020 mg/l, respectively. These are equivalent to approximately 4%, 10% and 13%, respectively, of the total lead initially present. For cement-A alone (no calcite) the extract concentrations and equivalent fractions are much lower at 9.0 mg/l (0.5%), 29.2 mg/l (0.7%) and 159.0 mg/l (2.0%) for 5%, 10% and 20% Pb-doped samples, respectively.

In comparison, very little lead is released from lead-doped materials solidified by cement-A to which calcite has been added. Leached lead concentrations range from 10.5 mg/l (0.1% of total lead) in Cal5,Pb10-A to below 0.01 mg/l (0.01% of total lead) for Cal10,Pb5-A. For cement-K, calcite addition results in more dramatic reduction in leached lead ranging from 57.0 mg/L (2.9% of total lead) for Cal10,Pb5-K, 41.9 mg/l (1.0% of total lead) for Cal10,Pb10-K and 432.0 mg/L (5.5% of total) for Cal5,Pb20-K.

3.5. SEM investigation

Electron microscopy images of the SWFs derived from the use of cement-A in the absence and presence of lead and in the absence and presence of calcite at 28 days of curing time are shown in Fig. 6. Hydration of cement-A is observed to be well

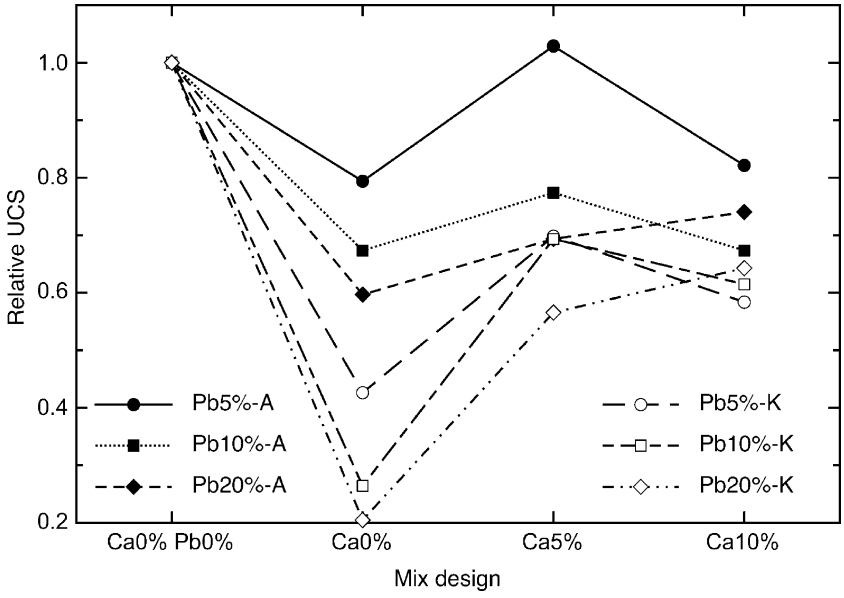

Fig. 4. Comparison of effect of calcite between A cement and K cement in the hydration of cement on UCS at 28 days.

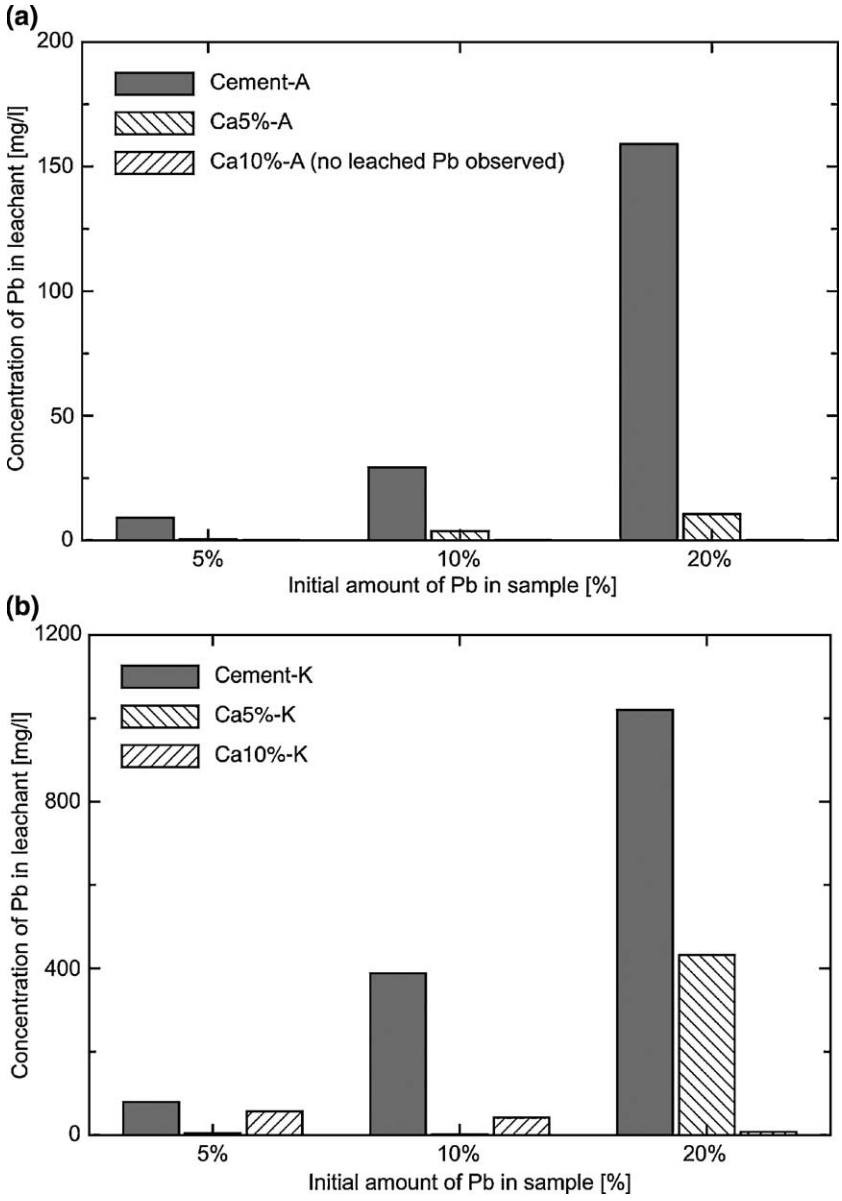

Fig. 5. Variation in leachability with calcite addition. (a) in Australian cement: (b) in Korean cement.

developed with silicate minerals in the cavity regions and extensive accumulations of needle-like ettringite ($3CaO{\cdot}Al_2O_3{\cdot}3CaSO_4{\cdot}32H_20$) produced by the hydration of C_3A in the presence of high gypsum content (see Fig. 6a). However, addition of 5% lead appears to produce coarse hydrated minerals with slightly more (plate-shaped) portlandite ($Ca(OH)_2$) and no silicate structure (see Fig. 6b).

An obvious difference in the absence and presence of calcite is the appearance of "coral-like" crystals of C–S–H including lead and plate-like crystals of portlandite as shown in Fig. 6c and d. In general, the presence of C–S–H and portlandite indicates a high degree of hydration development. Development of these crystals results in an increase in compressive strength and reduced leachability of Pb-doped SWF as shown in Figs. 3 and 5a. These "coral-like" crystals were also found in an SEM/EDS investigation of 20% lead-doped samples in the presence of 10% calcite within cavities after 28 days of curing. EDS analysis revealed that the coral-like crystals were principally of calcium lead silicate sulfate composition with measurable aluminium and iron contents [10].

Electron microscopy images of the solid matrix derived using cement-K with/without calcite and lead wastes at 28 days are shown in Fig. 7. Hydration development of regular cement-A produces C–S–H crystals and ettringite (Fig. 6a). In comparison, regular cement-K exhibits only C–S–H gel formation (Fig. 7a). The addition of lead to regular cement-K is observed to produce extensive accumulations of fragile substances (Fig. 7b). Addition of 5% calcite on lead doped materials SWF is found to again produce a well-developed C–S–H gel (Fig. 7c), and the addition of 10% calcite produces both C–S–H gel material and crystalline portlandite (Fig. 7d). It is evident therefore that addition of calcite to lead-doped materials induces acceleration in the hydration of both cement-A and cement-K [11].

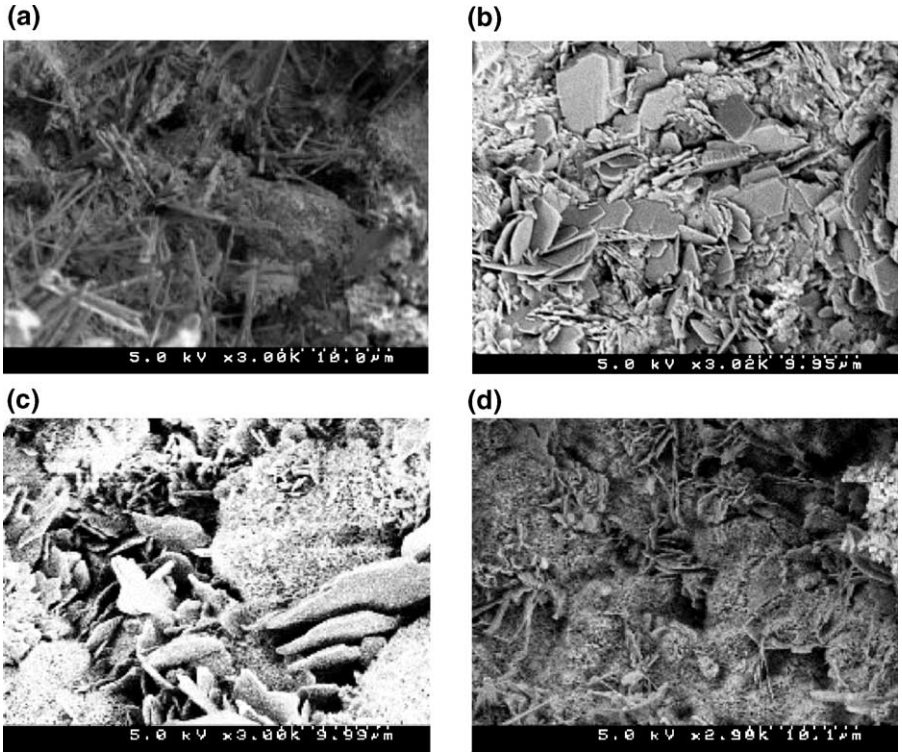

Fig. 6. SEM images of SWFs of Australian cement. (a) cement-A, (b) Pb5-A, (c) Cal5,Pb5-A, (d) Cal10,Pb5-A in a pore cavity at 28 days.

3.6. XRD investigation

3.6.1. Effect of calcite and lead in cement-K

X-ray diffraction patterns of the solid matrix of cement-K in the absence and presence of Pb and in the absence and presence of calcite at 7 days of curing time are shown in Fig. 8. An obvious difference in the images of lead-doped materials is the lack of diminution of OPC constituents (C_3S, C_2S, C_3A, C_4AF) and the apparent absence of portlandite ($Ca(OH)_2$) and C–S–H. In comparison, strong XRD peaks identified as C–S–H and C–S–H including Mg^{2+} and Al^{3+} (Sm and S2) are observed at 2θ values of 44.6°, 65.0° and 78.1° after 7 days of curing in

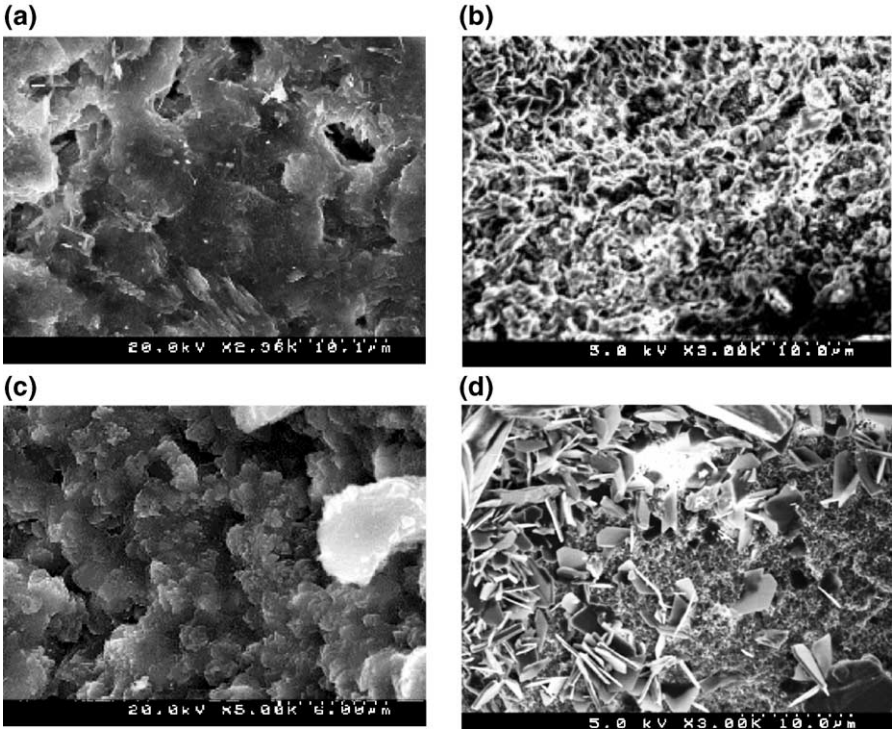

Fig. 7. SEM images of SWFs of Korean cement. (a) cement-K, (b) Pb5-K, (c) Cal5,Pb5-K, (d) Cal10,Pb5-K in a pore cavity at 28 days.

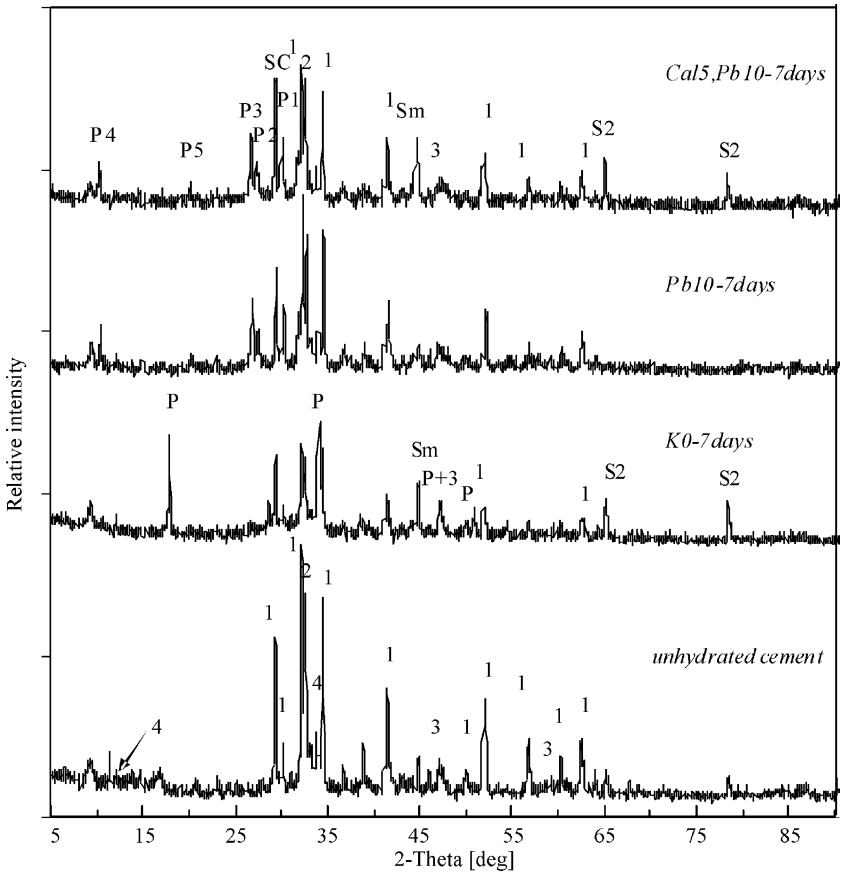

1	C_3S	P1	$Pb_2(NO_3)(OH)_3$	P	$Ca(OH)_2$
2	C_2S	P2	$Pb_4SO_4(CO_3)_2(OH)_2$	C	calcite
3	C_3A	P3	$3PbCO_3.2Pb(OH)_2.H_2O$(?)	S2	C-S-H (?)
4	C_4AF	P4	Pb wastes (1) (?)	Sm	C-S-H including Mg and Al
		P5	Pb wastes (2) (?)	SC	C3S+calcite(+C-S-H)

Fig. 8. XRD patterns of the SWF of cement-K at 7 days.

Cal5,Pb10-K as well as cement-K. This provides evidence for development of hydration in the presence of calcite, although the formation of portlandite is not apparent.

As investigated by Lee et al. [10], the XRD signature of the precipitated lead salt present in the initial synthetic waste ($Pb_2(NO_3)(OH)_3$) is also evident in the Pb-doped cemented solid as are a number of secondary precipitates presumably as a result of interaction of solubilized lead with sulfate from the OPC and carbonate anions from the atmosphere. In particular, there is evidence for the presence of lead carbonate sulfate hydroxide [$Pb_4SO_4(CO_3)_2(OH)_2$, JCPDS file No. 38–354], lead carbonate hydroxide hydrate [$3PbCO_3{\cdot}2Pb(OH)_2{\cdot}H_2O$, JCPDS file No. 9–356] and two other unidentified lead salts (P4 and P5).

It is clear from Fig. 9 that calcite addition to lead-doped materials solidified by cement-K markedly rectifies the poor hydration development with the formation of huge quantities of portlandite and C–S–H at 28 days compared to that in Pb10-K. Sm and S2 then disappear and are no longer evident in some samples after 28 days of curing. The reason for the transition of Sm and S2 after 14 days has not been established. It is a reasonable assumption however that, based upon the 28-day XRD results which show a marked disappearance of C_3S (34.4 $2\theta°$ and all other C_3S peaks) at 28 days, S2/Sm may be changed to other more silicate-rich C–S–H forms by more extensive polymerization. Calcite peaks in the XRD signatures are not identified on lead-doped material to which 5% calcite has been added in either the 7-day or 28-day samples. Lead-doped material in the absence of calcite is observed continually to induce considerable retardation in the curing process with the slow formation of portlandite and C–S–H, and with retention of P2 and P3 peaks.

3.6.2. Effect of lead and effect of calcite in cement-A

X-ray diffraction patterns of the solid matrix of materials formed using cement-A in the absence and presence of Pb and in the absence and presence of calcite at 7 days curing are shown in Fig. 10. Hydrated products of regular OPC on

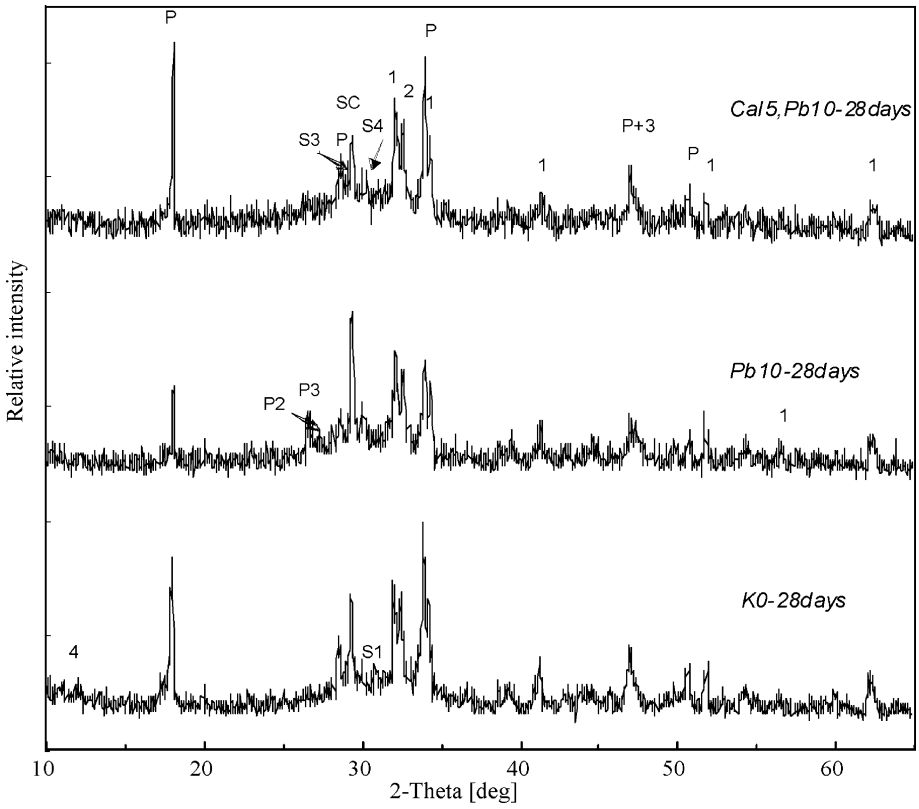

Fig. 9. XRD patterns of the SWF of cement-K at 28 days. S1: C–S–H, S2: calcium lead silicate, S4: calcium lead silicate sulfate hydroxide.

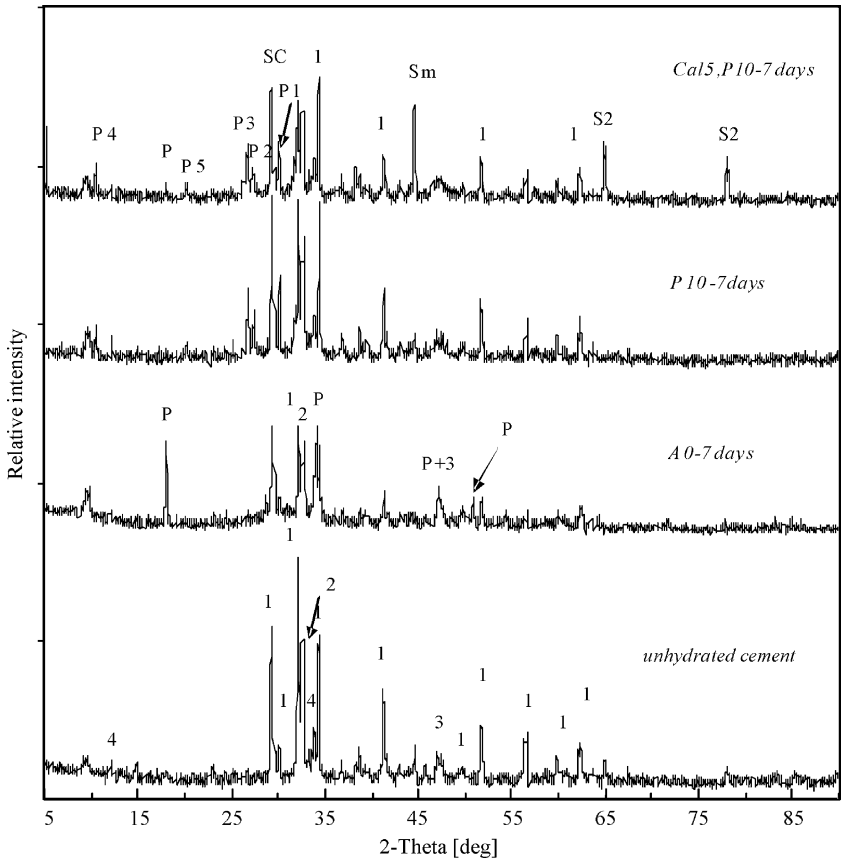

Fig. 10. XRD patterns of the SWF of cement-A at 7 days of curing time.

cement-A are observed to be similar to those on cement-K, but the S2 and Sm peaks of C–S–H are not apparent compared to their appearance in cement-K alone. We conclude that the initial form of the C–S–H gel is not responsible for the formation of the S2 and Sm peaks; rather, the formation of these phases can be attributed to other unidentified C–S–H forms including more silicate-rich components. This is based upon the early marked hydration development of regular cement-A (as confirmed by the significant diminution of OPC constituents (C_3S and C_4AF) and the formation of portlandite ($Ca(OH)_2$) and C–S–H gel after only 7 days of curing). This conclusion is also in accord with the hypothesis that the minerals contributing to the S2 and Sm peaks are transitory.

The presence of lead induces a marked retardation in hydration of the cementitious matrix as shown for cement-K at 7 days (Fig. 10d). There is also very little diminution of OPC constituents (C_3S, C_2S, C_3A, C_4AF) for these samples. The addition of calcite to lead-doped materials is observed to produce C–S–H peaks of S2 and Sm. There is also a slight formation of portlandite due to the acceleration of the hydration of cement components as confirmed by the marked diminution of C_4AF and the slight diminution of C_3S. The sharp and strong peaks indicative of the precipitation of lead secondary products (P2–P4) remain evident in both the absence and presence of calcite for lead-doped materials at 7 days (Fig. 10).

Strength development on OPC in the presence of lead is observed to recover after 28 days of curing time with almost the same peaks of all mineral products evident compared to regular OPC of cement-A as shown in Fig. 11. A small difference in the XRD spectra of the two samples is the evidence of remains of lead precipitates (slightly high P2 and a little P3) in Pb10-A. It is clearly evident that, in cement-A at 28 days, the presence of lead does not significantly retard cement hydration. The appearance of strong calcite peaks with high SC peaks and slightly increased portlandite on the addition of calcite to lead-doped materials in Cal5,Pb10-A is noteworthy.

3.7. Solution chemistry of cement–water systems

Comparison of the variations in concentrations of ions in cement–water solutions extracted from each cement-A and cement-K solidified sample in the absence and presence of lead and in the absence and presence of calcite over the 30 min after mixing at W/S=2 are shown in Table 5 and described briefly below.

CO_3^{2-}

Carbonate concentration in solution resulting from cement-A in the presence of lead is approximately two times higher than that of cement-K, and the concentration from cement-A in the absence of lead is slightly higher than that of cement-K. Higher concentrations of carbonate are observed in solutions contacting Pb-doped samples compared to the un-doped samples regardless of the presence of calcite in both cement-A and cement-K.

OH^-

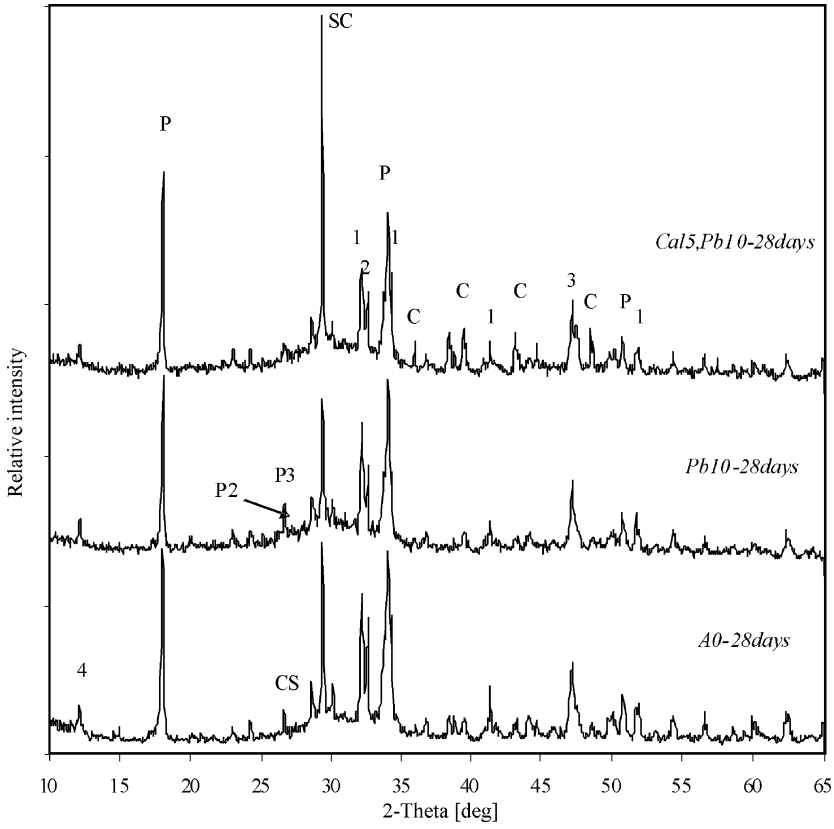

Fig. 11. XRD patterns of the SWF of cement-A at 28 days of curing time.

Table 5
Comparison of ionic concentrations (mM) of cement–water solution between cement-A and cement-K

	Time (min)	Ca	K	SO_4^{2-}	CO_3^{2-}	OH^-	Pb	pH
A0	2	24.8	46.5	2.1	2.7	83.2	0.0	12.92
	30	21.9	47.8	1.7	3.3	95.5	0.0	12.98
Cal5	2	34.9	55.2	2.7	3.7	89.1	0.0	12.95
	30	28.4	65.7	2.4	3.3	100.0	0.0	13.00
Pb10	2	24.9	40.7	1.6	6.6	75.9	11.6[a]	12.88
	30	21.6	39.6	1.9	6.2	79.4	4.1	12.90
Cal5,Pb10	2	34.9	49.1	2.4	13.2	81.3	13.1[a]	12.91
	30	31.9	55.8	2.3	12.1	91.2	6.0	12.96
K0	2	24.0	49.4	2.9	2.6	93.3	0.0	12.97
	30	19.6	50.6	2.2	1.8	120.2	0.0	13.08
Cal5	2	32.9	55.0	1.8	2.9	95.5	0.0	12.98
	30	27.4	53.5	1.7	2.9	128.8	0.0	13.11
Pb10	2	22.0	42.7	3.3	4.5	77.6	9.2[a]	12.89
	30	20.2	43.2	2.9	3.7	83.2	2.4	12.92
Cal5,Pb10	2	31.9	47.3	3.5	5.3	79.4	11.4[a]	12.90
	30	29.9	48.3	2.8	6.7	87.1	3.0	12.94

[a] Concentration of lead measured at 10 s.

The OH^- concentration in the cement-K and Cal5-K cases rises more sharply compared to that in the cement-A and Cal5-A. For K0 (cement-A), the pH of the solution exceeds 12.9 within the first few minutes and a similar result is evident for Cal5-K and A. The average OH^- concentration in the Pb-rich waste (Pb10) is somewhat reduced compared to samples without Pb in both cement-K and cement-A and may reflect the lowered rate of hydration of clinker components in this sample. Interestingly, despite the apparent ability of calcite to minimize the Pb-induced inhibition of hydration, the solution pH observed for Cal5,Pb10 is similar to the Pb-rich sample to which calcite was not added (Pb10). In addition, the [OH^-] of each sample of cement-K in the absence and presence of Pb and in the absence and presence of calcite is observed to be slightly higher than that of cement-A except for the Cal5,Pb10 samples.

Pb

The solution concentration of lead for both Pb10 and Cal5,Pb10 is initially around 9∼11 mM for cement-K and around 11∼13 mM for cement-A suggesting that solid lead precipitates present in the waste (mainly $Pb_2(NO_3)(OH)_3$) partially dissolve on mixing with the clinker slurry. There then follows a rapid decrease in solution concentration in lead, presumably reflecting the formation of secondary precipitates. The concentration of lead in solutions resulting from lead-doped samples for both cement-K and cement-A decreases markedly to 2∼3 and 4∼6 mM, respectively, though with a slightly higher concentration resulting from the sample to which calcite was added. Higher concentrations of lead are observed in solutions contacting cement-A to which lead waste was added compared to Pb-doped samples in cement-K.

Ca^{2+}

Calcium concentration in solutions of all samples of cement-A in the absence and presence of lead and in the absence and presence of calcite are slightly higher than those of cement-K. The calcium concentration in solutions in contact with solids to which calcite was added is slightly higher than non-calcite samples in both cement-K and cement-A.

SO_4^{2-}

Sulfate concentration in solutions resulting from samples of cement-A is lower than that of cement-K despite the high content of gypsum in cement-A. Higher concentrations of sulfate are observed in solutions contacting Pb-doped samples compared to un-doped samples in cement-K.

K^+

Potassium concentration in solutions extracted from cement-A is very similar to that from cement-K. The K^+ concentration in solutions resulting from samples to which Pb was added are lower than that in un-doped samples. The observation that K concentrations are higher in non Pb-doped samples is consistent with the results for ion concentrations in cement slurries reported by Thomas et al. [12]. The K^+ concentration in solutions resulting from samples to which calcite was added was found to be higher than that in non-calcite samples.

4. Discussion

4.1. Differences of effect of lead between cement-A and cement-K

A fixation model of lead wastes using cement-based S/S was developed by Lee et al. [10]. Lead wastes of lead nitrate hydroxide and lead oxide nitrate hydroxide dissolve within a few seconds generating dissolved Pb concentrations of up to 9∼13 mM in samples to which 10% lead had been added (Table 5). This dissolved Pb leads to formation of highly charged multinuclear species such as $Pb_6O(OH)_6^{4+}$ at the high pH typical of pore water solution [13].

These lead hydroxy-cations lead to the formation of extremely insoluble lead solids with sulphates and carbonates through the curing process of re-dissolution and precipitation. These salts are identified as lead carbonate sulfate hydroxide ($Pb_4SO_4(CO_3)_2(OH)_2$), lead carbonate hydroxide hydrate ($3PbCO_3{\cdot}2Pb(OH)_2{\cdot}H_2O$) and two other unidentified lead salts (P4 and P5) by XRD analysis (Figs. 8–11). These Pb salts (P1–P5) very slowly dissolve through the curing process and have virtually disappeared after 28 days. These Pb precipitates are located in the cavity areas and are readily accessible to leach water. Not surprising, they are very soluble under both highly acidic and highly basic conditions [14].

On the other hand, lead ions dissolved from the original Pb wastes not only form precipitates with sulphates and carbonate but also adsorb to silicate surfaces. A significant finding of our previous studies, using SEM/EDS/XRD [10] and EPMA [15], is the preferential deposition of lead as a membrane of lead species around cement clinker grains as well as lead precipitates in the cavity areas. The membrane of lead species selectively coats the clinker components, significantly blocking the hydration of these entities [13]. At the same time, as hydration is not completely stopped by the coating of Pb

species, diffusion processes through the coating are still active although at a reduced rate.

Dissolution of clinker materials will continue leading to an accumulation of ions in the pore waters of the kernel surrounded by the membrane. In the cavities outside the membrane, portlandite will precipitate as the pH rises leading to a reduction in the concentration of ions in solution. The difference in ionic concentrations on either side of the membrane leads to a significant osmotic pressure across the membrane which eventually leads to rupture of the membrane. Following equalisation of ionic composition on either side of the membrane, the coating reforms and the process of osmotic pressure build-up begins again.

Calcium ions are an extremely significant factor in the hydration of cement as well as in the periodic rupture of the membrane. The exact hydration rate depends on the reactivity of C_3S which is a provider of calcium ions to the pore water solution. It is accelerated with increasing amounts of SO_3 in cement and reduced with an increasing C_2S/C_3S ratio in the clinker.

From our model and other models mentioned above, it is possible to explain the different effects of lead fixation by cement-A and cement-K. Cement-A has a relatively higher ratio of C_3S, C_4AF and $CaSO_4$ compared to those of cement-K (Table 3). The higher concentration of calcium coming from C_3S in cement-A is trapped by the localized membrane, causing membrane rupture and re-formation of the membrane at the grain surface more frequently than in cement-K, thereby releasing hydrosilicate ions from within the membrane-bound core into the external solution. This induces not only hydration development of cement with the formation of condensed C–S–H and portlandite but also enhanced dissolution of lead precipitates (P1∼P5) with faster rupture of the membrane of lead species. In summary, cement-A is observed to have superior lead fixation ability and higher UCS due principally to its higher C_3S content compared to cement-K.

While lead-doped materials in cement-K have almost no compressive strength prior to 14 days of curing, the strength in cement-A is already up to 70% of that of cement-A at 14 days. Cement-A to which lead wastes were added also attains a ratio of relative UCS to regular OPC of 0.6–0.8 after 28 days of curing, but cement-K with lead addition has a UCS ratio (Pb-doped to regular) of only 0.2–0.4 (Fig. 4). The increasing UCS for cement-A in both the absence and presence of lead can likely be accounted by the higher C_3S content, as a provider of calcium ions in pore waters which induces the periodical rupture of the membrane, with increasing amounts of SO_3 and with a lower C_2S/C_3S ratio in the clinker.

Table 6 shows that the main cement components responsible for increased compressive strength are C_3S and C_4AF compared to that of C_2S and C_3A [16]. The lead concentration in pore waters of cement-A to which Pb wastes have been added is observed to be only 6.5%∼14.0% of that of cement-K. As a result, it is reasonable to conclude that regular cement-A has better fixation behaviour for lead in cement-based S/S than that of regular cement-K.

Table 6
Comparison of compressive strength on mineral composition of Portland cement [16]

	Compressive strength (kgf/cm^2)		
	7 days	28 days	1 year
C_3S	322	466	584
β-C_2S	24	42	325
C_3A	118	124	0
C_4AF	300	384	595

Electron microscopy and X-ray diffraction analyses give more evidence of the higher hydration development of cement-A associated with the more rapid rupture of the Pb-impregnated membrane. The higher hydration development in cement-A includes the faster dissolution of encapsulating membrane for the Pb-doped SWF (Pb10) compared to that of cement-K (Figs. 9 and 11). In addition, cement-A produces superior portlandite formation to that of cement-K. While electron micrographs of Pb10-A show the formation of significant amounts of portlandite in accordance with a greater degree of hydration, portlandite crystals are not evident in SWFs generated from Pb10-K.

Fixation of lead by the silicate arising from the hydration of C_3S has been well known in cement-based S/S. Bhatty [17] has argued that the lead is fixed into the cement matrix, forming a metallic calcium silicate hydrate in cement-based solidification. Some investigators found the metal hydroxide simply encapsulated in a silica matrix that prevents its removal [2,13]. Cocke [13] has shown (using XPS) that binding energies of lead ions are consistent with silicate, carbonate, or hydroxide compounds. It is likely that supersaturated solutions accumulated in the membrane at the reduced rate of hydration produce new precipitate with re-dissolved Pb species from P1∼P5. These new precipitates are gel-like and may be represented by the non-stoichiometric formula C–Pb–S–H. The micrographs and chemical compositions of these C–Pb–S–H gels have been described previously following investigations using SEM/EDS [10] and EPMA [15].

4.2. Differences of S/S effect of calcite between cement-A and cement-K

The concentration of calcium ions in the cement–water solution to which calcite has been added is observed to be higher than in the case of non-calcite addition (Table 5). The results are consistent with the proposal by Nehdi and Mindess [11] that the presence of calcite removes calcium ions from the cement–water solution from earlier curing, and strongly promotes further dissolution of calcium ions through the hydration membrane formed around the cement gains. This subsequently enhances the dissolution of C_3S to restore the equilibrium between solutions on either side of the hydration membrane.

The accelerating effect of calcite in the hydration of C_3S has been argued by many researchers. Ramachandran and Zhang [18] found that the addition of calcite accelerates the hydration of C_3S, and as much as 25% of added calcium carbonate was

incorporated into the C–S–H phase within three days. Sharma and Pandey [19] also investigated the accelerating effect of C_3S and C_2S hydration in the presence of the fine calcite particles by differential thermal analysis. The broadening of endotherms at 140–180 °C in calcite-doped samples indicates the presence of a higher amount of combined water associated with increased amounts of calcium silicate hydrate and other hydrated minerals. Soroka and Stern [20] argued that calcite plays a significant role as inert microfiller, which accelerates the cement hydration through increased nucleation. Nucleation and growth mechanisms promote early hydration and hydration products may preferentially nucleate on calcite particles [21].

Calcite addition in the presence of lead induces a marked dissolution of calcium ions compared to Pb-doped SWF with no additional calcite (Table 5). The increasing germination of portlandite with the removal of Ca^{2+} and OH^- in the presence of calcite accelerates the osmotic driving force and hence promotes the rupture of the insoluble membrane of lead species that engulfs the cement grains [21]. As a result, at the early stage of hydration, calcite addition enhances the crystallization of portlandite coincident with the onset of C–S–H germination in the presence of lead as well as in the absence of lead.

The increasing germination of portlandite and C–S–H on calcite addition enhances the development of compressive strength in lead-doped materials. The different effects of calcite between cement-A and cement-K can be deduced from the X-ray diffraction results. While peaks of portlandite in Pb10-K are markedly lower than those in regular cement-K due to the retardation effect of lead, the peaks in Cal5,Pb10-K are approximately 2~3 times higher than those of Pb10-K (Fig. 9). However, in cement-A, portlandite peaks of Cal5,Pb10-A are similar to those of Pb10-A.

Calcite addition to lead-doped materials (C5P10) is also observed to enhance the dissolution of lead precipitates (P1~P5) with the development of early hydration compared to that of non-calcite samples (Pb10). While the X-ray diffraction peaks of P2 and P3 in Pb-doped SWF with non-calcite addition are still high at 28 days, the peaks in Pb-doped SWF with calcite addition almost disappear with significant decrease of peaks of C_3S (41.3 $2\theta°$, 51.8 $2\theta°$, etc.) shown in Figs. 9 and 11. The decrease of lead precipitate peaks by the addition of calcite provides evidence of the improved immobilization of lead because the Pb precipitates in the cavity area are more accessible to leach water and are apparently more soluble under the strong acidic conditions of the leachant [14].

The addition of calcite is observed to enhance polymerization of C–S–H including lead ions, producing the “coral-like” crystals of C–Pb–S–H in cement-A (Fig. 6c and d) and in cement-K (Fig. 7d). The chemical compositions of these materials have been identified by SEM/EDS [10] as calcium lead silicate sulfate (probably hydroxide) with elevated levels of aluminium and iron. It is apparent the structure of C–Pb–S–H is more stable under the strong acidic conditions of leaching on the surface of Pb-doped SWF than the coarse and fragile minerals of Pb10-A (Fig. 6b) and Pb10-K (Fig. 7b). C–Pb–S–H solids in cement-A are observed to be more resilient than those in cement-K. In addition, immobilization of lead in the presence of calcite on leaching is more effective in cement-A due to enhanced crystalline structure of C–Pb–S–H than is the case in cement-K.

Interestingly, a large number of strong peaks of calcite (36.1, 39.5, 43.3, and 48.6 $2\theta°$) are observed in Cal5,Pb10-A at 28 days of curing (Fig. 11). However, no specific peaks of calcite are found in any cement-A samples at 7 days or in any cement-K samples at 7 and 28 days of curing. Therefore, the presence of calcite in Cal5,Pb10-A is apparently not original calcite added before curing but new crystals formed during curing. It is assumed that new calcite apparent after 28 days of curing is formed as a result of the very high CO_3^{2-} concentration (at least 2~4 times higher than that of other samples) in the cement–water solution in equilibrium with portlandite [22]:

$$Ca(OH)_2(s) + CO_2 \rightleftharpoons CaCO_3(s) + H_2O$$

It is also well known that carbonation of C–S–H gel, the other major cement hydration product, results in the formation of calcite [23,24]:

$$C - S - H + CO_2 \rightleftharpoons CaCO_3(s) + \text{silica} + H_2O$$

5. Conclusions

In this study, we have examined the differences in the effect of calcite on the strength and stability of Pb-rich wastes solidified and stabilized using Australian and South Korean ordinary Portland cements. Pb-rich waste stabilized using Australian OPC has been shown to possess both substantially higher unconfined compressive strength and lead immobilization ability (as gauged by leachability studies) than South Korean OPC as a result of its higher C_3S content and the associated enhanced degree of precipitation of lead on the surfaces of silicate phases present.

Calcite addition is observed to have an accelerating effect on the OPC-induced solidification/stabilization of Pb-rich wastes as gauged by the unconfined compressive strength and leachability of the solids formed. This effect is observed to be far more dramatic for South Korean OPC than for Australian OPC with the Korean OPC-solidified Pb-rich wastes exhibiting much lower UCSs than Australian OPC-solidified Pb-rich wastes but the strengths being comparable (after 60 days of curing) on addition of 10% by weight of calcite.

Using scanning electron microscopy, waste stabilized with cement and calcite was observed to develop significantly greater proportions of hydrated crystals than wastes stabilized with cement alone. The results of X-ray diffraction studies have shown that the presence of calcite in South Korean OPC results in greater acceleration in the formation of portlandite than is the case for Australian OPC.

References

[1] M.D. LaGrega, P.L. Buckingham, J.C. Evans, Hazardous Waste Management, McGraw-Hill, Inc., New York, 1994.

[2] J.R. Conner, Chemical Fixation and Solidification of Hazardous Wastes, Van Nostrand Reinhold, New York, 1990.
[3] S.K. Lee, D.K. Lee, D.J. Lee, Y.P. Park, S.M. Lee, J. Korean Solid Wastes Eng. 16 (5) (1999) 451.
[4] Y. Arai, Semento no Zairyo Kagaku, Dainippon Tosho Pub., Japan, 1990.
[5] M. Murat, F. Sorrentino, Cem. Concr. Res. 26 (3) (1996) 377.
[6] L.C. Lange, C.D. Hills, A.B. Poole, J. Hazard. Mater. 52 (1997) 193.
[7] R.K. Vempati, M.Y.A. Mollah, A.K. Chinthala, D.L. Cocke, Waste Manag. 15 (5/6) (1997) 433.
[8] www.epa.gov/epaoswer/hazwaste/test/1xxx.htm.
[9] American Public Health Association, American Water Works Association, Water Environment Federation, in: A.D. Eaton, L.S. Clesceri, A.E. Greenberg, et al. (Eds.), Standard Methods for Examination of Water and Wastewater, 19th eds., American Public Health Association, Washington, DC, 1995.
[10] D. Lee, G. Swarbrick, T.D. Waite, Cem. Concr. Res. 35 (2005) 1027.
[11] M. Nehdi, S. Mindess, in: Y. Skalny, S. Mindess (Eds.), Materials Science of Concrete, American Ceramic Society, 2000, p. 49.
[12] N.L. Thomas, D.A. Jameson, D.D. Double, Cem. Concr. Res. 11 (1981) 143.
[13] D.L. Cocke, J. Hazard. Mater. 24 (1990) 231.
[14] F.K. Cartledge, L.G. Butler, D. Chalasani, H.C. Eaton, F.P. Frey, E. Herrera, M.E. Tittlebaum, S.L. Yang, Environ. Sci. Technol. 24 (6) (1990) 867.
[15] D. Lee, T.D. Waite, J. Hazard. Mater., submitted for publication.
[16] F.M. Lea, The Chemistry of Cement and Concrete, Edward Arnold Ltd, Glasgow, UK, 1970.
[17] M.S.Y. Bhatty, Superfund 87 (1987) 140.
[18] V.S. Ramachandran, C. Zhang, Durab. Build. Mater. 4 (1986) 45.
[19] R.L. Sharma, S.P. Pandey, Cem. Concr. Res. 29 (1999) 1525.
[20] I. Soroka, N. Stern, Cem. Concr. Res. 6 (1976) 367.
[21] M. Nehidi, Cem. Concr. Res. 30 (2000) 1663.
[22] M. Eglinton, in: P.C. Hewlett (Ed.), Lea's Chemistry of Cement and Concrete, Arnold Pub. Ltd., London, 1998, p. 241.
[23] M. Yousuf, A. Mollah, T.R. Hess, Y.-N. Tasi, D.L. Cocke, Cem. Concr. Res. 23 (1993) 773.
[24] E.J. Reardon, B.R. James, Cem. Concr. Res. 19 (1989) 385.